MEASUREMENT SCIENCE REVIEW, **23**, (2023), No. 1, 40-46

sciendo

ISSN 1335-8871

MEASUREMENT SCIENCE REVIEW

Journal homepage: https://content.sciendo.com

Equivalence Ratio Modelling of Premixed Propane Flame by Multiple Linear Regression Using Flame Color and Spatial Characteristics

Hao Yang[1], Yufeng Lai[2], Xuanqi Liu[3], Houshi Jiang[4], Jiansheng Yang[1*]

[1]*The Electrical Engineering College, Guizhou University, Guiyang, China, jsyang3@gzu.edu.cn*
[2]*Department of Electronic and Electrical Engineering, The University of Sheffield, Sheffield, United Kingdom*
[3]*Department of Mechanical Engineering, The University of Sheffield, Sheffield, United Kingdom*
[4]*School of Mechanical Engineering, Beijing Institute of Technology, Beijing, China*

Abstract: Equivalence ratio (Φ) is one of the most important parameters in combustion diagnostics. In previous studies, flame color characteristics have been widely applied to model the Φ of premixed hydrocarbon flames. The flame spatial characteristics also change with the varying Φ. In this paper, a high-speed color camera was employed to capture the premixed propane flame images under different Φ conditions (Φ = *0.93 to 1.53*). Then, the relationship between the spatial characteristics and the Φ variation was investigated. The area and height of propane premixed flames perform a strong sensitive response to the Φ variation. Based on the research above, the Φ measurement models were constructed using color and spatial characteristics. A comparison was made between the color characteristics (*Color*-Φ) model and the color-spatial characteristics (*Multi-dimensional*-Φ) model. Both models were applied to a set of color images of a premixed propane flame, and the result indicates that the *Multi-dimensional*-Φ model performs with higher accuracy.

Keywords: Combustion diagnostics, equivalence ratio modelling, flame color characteristic, flame spatial characteristic, multiple linear regression

1. INTRODUCTION

Combustion diagnostics is one of the biggest challenges the combustion industry faces. It is a technique that applies different methods to diagnose the process of flame combustion, such as combustion rate, stability, equivalence ratio, pollutant emissions, etc. Among the above parameters, the equivalence ratio [1] is a physical quantity that measures the mixing degree of fuel and oxidizer, which has a great impact on the combustion state and the pollutant emissions. Therefore, the accurate equivalence ratio (Φ) measurement is of great importance for the combustion industry to improve energy efficiency and reduce pollutant emissions.

The flame exhibits different spectral and spatial characteristics under different combustion conditions. The property of radical chemiluminescence emission is one of the spectral characteristics that have been used for the Φ measurement of flames. For hydrocarbon flames, the specific radicals emit the photons at certain wavelengths, such as the peak of OH^* at 310 nm [2]. This shows that the Φ can be measured according to these chemiluminescence peaks. The OH^* chemiluminescence intensity can be used to indicate the global Φ, since the OH^* emission intensity increases with the increasing Φ [3]. It has been shown that the chemiluminescence intensities of CH^* and C_2^* also change with the Φ of flames non-monotonically [4]. Clark [5] also investigated that the CH^*/C_2^* ratio can be used to indicate the Φ of propane-air flames under conditions (Φ = *0.6 to 1.5*).

For the analysis of the radical emission spectrum, spectroscopy is the most accurate method providing detailed spectral information about the target flame area [6]. However, the radical spatial information cannot be directly obtained from spectroscopy, thus the flame structure and local Φ can hardly be analyzed. To analyze the radical spatial information, some researchers used a multispectral imaging method to capture the flame radical images, which can provide both spectral and spatial information [7]. The common method used is to apply the specific narrowband filters in combination with a camera, and the flame radical emissions at different wavelengths are imaged accordingly [3]. The other common method used is to apply the narrowband filters with different specific bands to several cameras, and the flame radical emissions at different wavelengths are imaged at the same time. Since the different flame radical emissions cannot be obtained simultaneously by one camera, one challenge of this method is to precisely synchronize the images captured by different cameras.

DOI: 10.2478/msr-2023-0005

Corresponding author: jsyang3@gzu.edu.cn *(J. Yang)*

Therefore, a low error of integration time and low lens distortion is required for the instruments.

Flame color can be seen as a representation of the flame spectrum, hence the researchers are concerned with the color modelling method. Huang et al. [8] found that the average intensities of the Blue (B) and Green (G) channels of a methane-air premixed flame color image were well matched with the chemiluminescence intensities CH^* and C_2^*. Then, the Φ can be measured by modelling with the color B/G in the flame image. However, each pixel of the color image is interpolated with a Bayer filter. Additionally, the *RGB* band is broad, and the image color is integrated from the broadband. Thus, the color modelled method proposed by Huang et al. [8] loses a certain spectral resolution. In this case, the image color contains a lot of redundant spectral information. Therefore, the accuracy of the chemiluminescence intensity measured by the color method is not precise enough. To increase the accuracy of Φ measurement by image color, Yang et al. [9] proposed an improved color model by considering the spectrum response of the camera image sensor.

The conventional color modelled Φ measurement method considers only the flame color information. Both color and spatial characteristics change with varying Φ. For the same type of air-fuel premixed flame, the air volume and oxygen content affect the length of the flames [1]. In addition, for fuel with a different chemical ratio between the hydrogen and carbon atoms, the flame height increases when the chemical ratio between hydrogen and carbon atoms of the fuel decreases under the same conditions. For example, the flame length of propane is approximately 2.5 times longer than that of methane [1]. It is more effective and practical to have the optimal combination of correlated variables to predict or estimate the independent variable. Thus, the combination of color and spatial characteristics seems to be more effective and practical to estimate Φ.

The rapid advances in machine learning offer new technical methods for modelling high-dimensional data. Machine learning algorithms can fit not only high-dimensional linear data but also non-linear data. In this case, the machine learning algorithm can be applied to construct the Φ model based on both color-spatial characteristics. In the previous studies, Ge et al. [10] analyzed the spectrum of the biomass flame over the spectral wavelength from 200 nm to 1200 nm. And the spectral peak intensities of OH^* (310.85 nm), CN^* (390.00 nm), CH^* (430.57 nm), and C_2^* (515.23 nm, 545.59 nm) were extracted as the characteristics of the biomass flame. After the characteristic extraction, Ge et al. [10] constructed the identification model including decision tree [11], and random forest [12], and realized the goal of type identification of the biomass fuel. Wang et al. [13] extracted the total area, gray value, averaged intensity of B channel, etc. as the characteristics of a gas fire. Then, fuzzy pattern recognition was employed to identify the combustion state under varying Φ conditions. Machine learning has been applied in combustion diagnostics as mentioned above, but it has not been employed in Φ measurement.

In this work, we studied both color and spatial characteristics for modelling of Φ. The relationship between varying Φ and spatial characteristics was investigated, then the area and height of the flame were extracted as spatial characteristics. The intensity of the B Channel and the G Channel, the B/G ratio, and the improved color modelled CH^*/C_2^* ratio proposed by Yang et al. [9] were extracted as the color characteristics. Since there is multicollinearity among these characteristics in the same space, we used the characteristic selection method to choose the characteristics. Multiple Linear Regression (*MLR*) was applied to establish the relationship between both color-spatial characteristics and Φ. At last, a comparison was investigated between the color characteristics (*Color-Φ*) model and the *Color-spatial-Φ* model.

2. METHODOLOGY

A. Experimental setup

In this work, we performed Φ measurement on premixed air-propane flames and the inner nozzle diameter of the Bunsen burner was 10 mm. The Photron FASTCAM SA-4 high-speed color camera with a Sigma 24-70 nm, f/2.8 EX DG zoom lens was used to capture the flame images, as shown in Fig. 1. The Φ of the flame was increased from 0.93 to 1.53 at intervals of 0.1 L/min of air flow rates and the fuel flow remained at 0.105 L/min across 12 cases. For each set of Φ, 2000 images were captured at the steady combustion state. The combustion and imaging system was used in the improved color modelled CH^* and C_2^* measurements [9].

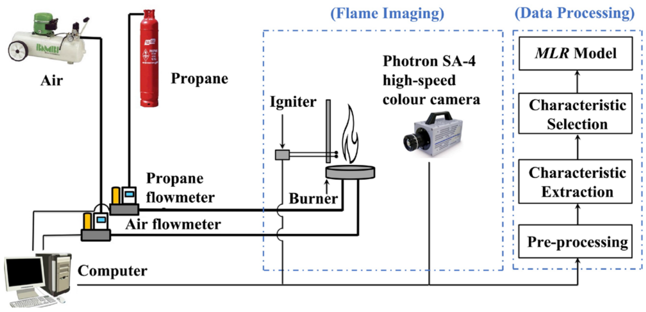

Fig. 1. Experimental setup and block diagram for Φ measurement based on *MLR*.

After the data acquisition was completed, the flame color images needed pre-processing for noise reduction. Then the spatial and color characteristics were extracted for further analysis. Based on this, the *MLR* models were constructed with different combinations of characteristics, and the model with better performance in the evaluation indices was selected as the color-spatial characteristics (*Multi-dimensional-Φ*) model.

B. Data pre-processing

The acquired image data are shown in Fig. 2 (upper). The original flame image was processed by the Gaussian filtering algorithm with a 5×5 Gaussian kernel for noise reduction. The brightness and contrast of the color images were enhanced by 40 percent for visualization. Fig. 2 presents the enhanced flame images. It is found that the color of the flame changes from blue to greenish-blue, which is caused by the increase of C_2^*/CH^* in the combustion progress. The spatial characteristic parameters such as height, area, etc. have changed due to the variation of flow speed, different combustion processes and different spatial distribution of fuel.

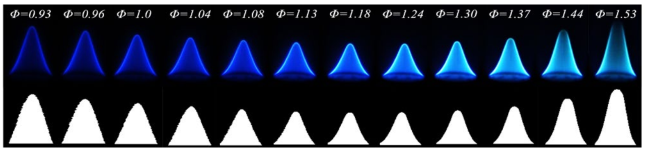

Fig. 2. The segmented flame profiles (upper) and flame segmentation (lower) at conditions (*Φ = 0.93 to 1.53*).

Then, the Otsu segmentation algorithm and the Canny edge detection algorithm were combined to segment the contours of the flames to improve the accuracy of the segmentation. As shown in Fig. 2, the actual area of the flame should be calculated from the bottom part of the flame above the nozzle, which is also the widest part of the flame. Based on this, we select the widest part as the bottom of the flame to further improve the accuracy of the segmentation algorithm, and the flame segmentation result is presented in Fig. 2 (lower). The relationship between varying *Φ* and variation of spatial characteristic parameters can be intuitively studied from the segmentation result. Abel transform was performed for all image data to transform the images from cylindrical to 2D, and the transformed result is shown in Fig. 3.

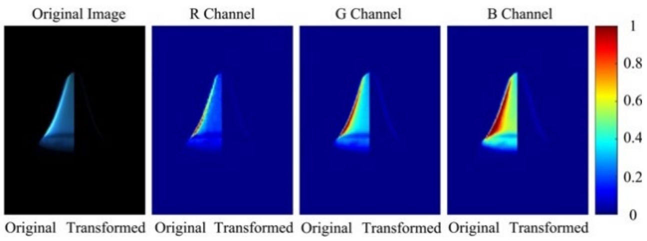

Fig. 3. The original and Abel transformed image.

C. Color and spatial characteristics extraction

The accuracy of the *MLR* model for the color-modelled *Φ* measurement is strongly dependent on the quality of characteristics extracted from the flame color images. The more sensitively characteristics change with the variation of *Φ*, the more discriminatory the characteristics are. The following section provides the definition and mathematical expression of the characteristics in color and spatial dimension.

The spatial characteristics of flames consist of the geometrical parameters that vary with the increase of *Φ*. The total area of the flame represents the sum of the pixels of the flame in the color image as in (1) and (2).

$$P_f(x, y) = \begin{cases} 1, & \text{if } G(x, y) > \lambda \\ 0, & \text{other} \end{cases} \tag{1}$$

$$A_f = \sum_{x \in f} \sum_{y \in f} 1 \tag{2}$$

Here, (x, y) indicates the pixel point in the flame image and $G(x, y)$ represents the gray scale of the pixel point. λ denotes the gray scale threshold. $P_f(x, y)$ represents the binarization result of the pixel point (x, y). P_f is equal to 1 if $G(x, y) > \lambda$, and P_f is equal to 0 if $G(x, y) < \lambda$ or $G(x, y) = \lambda$. A_f shows the total area of the flame and is the sum of $P_f(x, y)$, which is equal to 1.

In addition, the flame height also changes with the variation of *Φ*. Therefore, the correlation between *Φ* and height is investigated. The height of the flame in the image is defined as:

$$H_f = \max\left(y \middle| P_f(x, y) = 1\right) - \min\left(y \middle| P_f(x, y) = 1\right) \tag{3}$$

where Hf represents the flame height. The correlations between *Φ* and spatial characteristics extracted are plotted in Fig. 4. In addition, the global width of the flame changes with varying *Φ*, which is shown in Fig. 2. However, the definition of the flame width is ambiguous because the width of the different flame parts is different. And the bottom width of the flame is determined by the nozzle, which does not change with varying *Φ*. Moreover, the variation of the area already includes the combination of varying height and width. Based on the above, we did not extract the flame width as a spatial characteristic.

The greenish-blue flame color is attributed to radical chemiluminescence. Therefore, color is the main characteristic of a premixed propane flame, which contains the integration of spectral information of radicals over the broad wavelength. According to the study of Huang et al. [8], the chemiluminescence intensities of CH^* and C_2^* are well matched with the averaged intensities of the *B* and *G* channels in the premixed methane flame image. Based on this, the averaged intensities of the *B* and *G* channels in premixed propane flame images are extracted as color characteristics. The averaged intensities of the *B* and *G* channels denote the average intensity of the *B* and *G* channels of all pixels occupied by the flames in the color images defined as (4) and (5). Yang et al. [9] illustrated that the ratio of the average *B* and *G* intensities can be used approximately to indicate the *Φ* of the flame. Therefore, *B*/*G* can also be extracted as the characteristic defined as (6). Finally, the improved color modelled CH^*/C_2^* ratio proposed by Yang et al. [9] was used as the characteristic, shown as (7).

$$I_B = \frac{1}{K} \sum_{(x,y) \in f} B_p(x, y) \tag{4}$$

$$I_G = \frac{1}{K} \sum_{(x,y) \in f} G_p(x, y) \tag{5}$$

$$T_f = \frac{\sum_{(x,y) \in f} B_p(x, y)}{\sum_{(x,y) \in f} G_p(x, y)} \tag{6}$$

$$I_f = \frac{3.03 \sum_{(x,y) \in f} B_p(x, y) - 3.3 \sum_{(x,y) \in f} G_p(x, y)}{1.79 \sum_{(x,y) \in f} G_p(x, y)} \tag{7}$$

where the I_B and I_G represent the averaged intensities of the *B* and *G* channels, respectively. T_f is the averaged intensity ratio of the *B* and *G* channels and I_f is the improved color-modelled CH^*/C_2^* ratio. *K* denotes the sum of pixels occupied by the flame. $B_p(x, y)$ and $G_p(x, y)$ indicate the intensity of the *B* and *G* channels of the pixel point (x, y), respectively.

3. Results and discussion

A. *Color and spatial characteristic analysis*

For each set of Φ, 100 sets of data are extracted for each dimensional characteristic, giving a total of 1200 sets of data. The 100 sets of data are averaged for each set of Φ to illustrate the trend of the characteristics corresponding to the variation of Φ from 0.93-1.53 and plotted in Fig. 4 and Fig. 5. The standard deviation (σ) is applied to assess the fluctuations of each 100 sets of data to ensure the accuracy of the characteristic data, which are shown as red lines in Fig. 4 and Fig. 5.

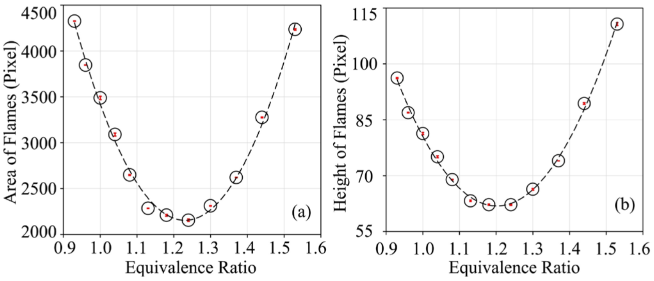

Fig. 4. The correlation between Φ and spatial characteristics of flames. (a) relationship between A_f and Φ. (b) relationship between H_f and Φ.

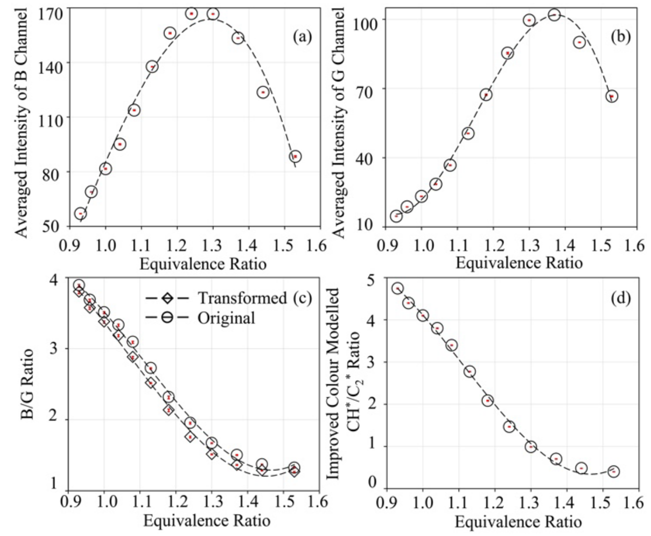

Fig. 5. The relationship between Φ and color characteristics of flames. (a) relation between I_B and Φ. (b) relationship between I_G and Φ. (c) relationship between T_f, Abel transformed T_f and Φ. (d) relationship between T_f and Φ.

As shown in Fig. 4(a), A_f decreases rapidly under conditions (*Φ = 0.93 to 1.24*) and increases under conditions (*Φ = 1.24 to 1.53*). The variation trend of H_f is plotted in Fig. 4(b) that the H_f decreases under conditions (*Φ = 0.93 to 1.24*) and increases under conditions (*Φ = 1.24 to 1.53*). This indicates that the variation of A_f and H_f is sensitive to the varying Φ conditions, and the varying trend of A_f and H_f under conditions (*Φ = 0.93 to 1.24* and *Φ = 1.24 to 1.53*) is separately approximately linear. The *MLR* model is a linear model that requires the relationship between independent and dependent variables. Therefore, both A_f and H_f can be employed in the *MLR* model. In addition, as seen from Fig. 4, the standard deviations of A_f and H_f are small, which ensures the accuracy and stability of the model.

The correlations between Φ and the color characteristics extracted from flames are plotted in Fig. 5. Fig. 5(a) illustrates the variation trend of I_B with the increase of Φ. It can be found that I_B increases under conditions (*Φ = 0.93 to 1.24*) and decreases under conditions (*Φ = 1.24 to 1.53*). This is similar to the variation trend of I_B, I_G that increases under conditions (*Φ = 0.93 to 1.37*) and decreases under conditions (*Φ = 1.37 to 1.53*) as plotted in Fig. 5(b). Fig. 5(c) and Fig. 5(d) show that the T_f and I_f keep decreasing under experimental conditions (*Φ = 0.93 to 1.53*).

Additionally, the Abel transformed *B/G* ratio was plotted in Fig. 5(c). It shows that there is no obvious difference between the *B/G* ratio and the Abel transformed *B/G* ratio. This is because the flames used in this study are uniform along the flame sheet. And the normalization of the *B/G* ratio is the same as that of the Abel transformed *B/G* ratio due to their similar trend.

B. *Multi-dimensional-Φ and Color-Φ modelling*

All data were normalized to remove the dimension of the data and to eliminate the residuals caused by the data acquisition. The Φ measurement model based on *MLR* was constructed separately under combustion conditions (*Φ = 0.93 to 1.24* and *Φ = 1.24 to 1.53*). In this equation, Y is the Φ of the premixed propane flame and X denotes a vector of N characteristics, and the models are formed as:

$$Y = \beta_0 + \sum_{n=1}^{N} \beta_n X_n + \varepsilon \tag{8}$$

where X_n is the characteristic n which is an independent variable. The β_0 is a common intercept and β_n denotes the regression coefficient of characteristic n. The ε is the random error that is assumed to follow the normal distribution with mean zero and standard deviation σ.

Severe multicollinearity between the independent variables makes the regression model unstable and the model calculations unreliable, so the data are analyzed separately for spatial and color variables before model construction. The variance inflation factor (*VIF*) and correlation coefficient (*Corr*) were used to verify the correlation among the characteristics extracted as (9) and (11). The correlation coefficients between the variables were first determined on a case-by-case basis using *Corr*. After completing the pre-processing of the data, *VIF* was used to further determine that there was no severe multicollinearity between the variables. Mean absolute error (*MAE*) was applied to evaluate the error between the calculated and true values of the model, which is formed as (12).

$$VIF = \frac{1}{1 - R^2} \tag{9}$$

$$R^2 = 1 - \frac{\sum_{i=0}^{n} (y_i - f(x_i))^2}{\sum_{i=0}^{n} (y_i - y_a)^2} \tag{10}$$

$$Corr\,(a, b) = \frac{Cov\,(a, b)}{\sqrt{Var\,(a) \cdot Var\,(b)}} \tag{11}$$

$$MAE = \frac{1}{n}\sum_{i=0}^{n}|y_i - f(x_i)| \tag{12}$$

where R^2 denotes the coefficient of determination as (10), *Cov* (a, b) indicating the covariance of a and b, and *Var* (a, b) indicating the variance of a and b. In (10) and (12), n is the sum of data, y_i and $f(x_i)$ denoting separately the true and calculated value, y_a denoting the averaged value of y_i.

The correlation coefficient between the extracted characteristics is plotted separately in Fig. 6 under combustion conditions ($\Phi = 0.93$ *to* 1.24 and $\Phi = 1.24$ *to* 1.53). This indicates the correlation between the two variables is nearly linear when the absolute correlation coefficient is exactly 1 between the two variables. In other words, it demonstrates that the two variables can be expressed by each other in an approximately linear correlation with a correlation coefficient approximating exactly 1.

Similarly, for the color characteristics, there is severe collinearity between T_f and I_f, and thus the two color characteristics cannot appear in the same linear model at the same time. In addition, there is severe multicollinearity between I_B and I_G in both conditions. Since T_f and I_f are ratios based on I_B and I_G, T_f and I_f already contain the information of I_B and I_G. Therefore, there is severe multicollinearity between T_f, I_f, and I_B, I_G. Because T_f and I_f already contain the information of I_B and I_G, T_f, I_f show an approximately linear trend under conditions ($\Phi = 0.93$ *to* 1.53). Thus, T_f and I_f are more suitable for the linear regression model compared with I_B and I_G. Based on the above, T_f and I_f were selected as the color characteristics of flames.

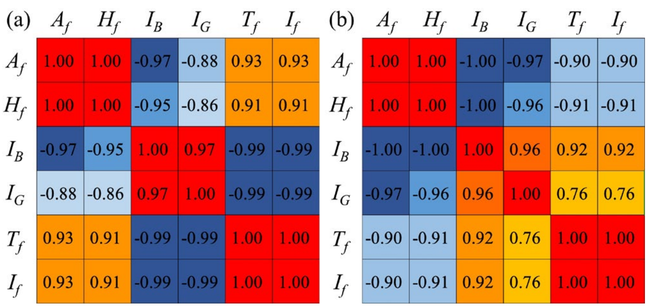

Fig. 6. Correlation coefficients. (a) $\Phi = 0.93$ *to* 1.24. (b) $\Phi = 1.24$ *to* 1.53.

Overall, Fig. 6 indicates that the multicollinearity between spatial and color characteristics is considerable. However, in reality, spatial and color characteristics change simultaneously along with the variation of Φ, so the multicollinearity between these two different dimensional characteristics will be further determined using *VIF* when constructing the model. There is severe multicollinearity between variables a and b when absolute $VIF > 10$, as shown by Mason et al. [15].

Due to the presence of severe multicollinearity among the characteristic variables, this paper employs the characteristic selection method, which draws on the idea of stepwise selection [16] to construct the Φ model. The stepwise selection was used to select the different characteristics to construct the regression model. One independent variable at a time is initially introduced for testing, and then the other independent variables are gradually introduced. Then, all variables are tested, and if the originally introduced variables become less significant due to later introductions, they are removed accordingly. The optimal regression equation is gradually obtained.

Drawing on the idea of stepwise selection, a characteristic variable in the spatial space is introduced first, then a characteristic in the color space is selected for model construction. Then, the characteristics introduced are tested for significance and *VIF*. The color characteristic variable will be removed if it is not significant or if there is multicollinearity between the spatial and color characteristics. The optimal Φ regression model is gradually obtained.

The Φ measurement models were constructed under two different combustion conditions ($\Phi = 0.93$ *to* 1.24 and $\Phi = 1.24$ *to* 1.53). One spatial characteristic is introduced first, followed by color characteristics in turn, and significance tests and *VIF* tests are performed. The model constructed with characteristic selection is shown in Table 1 ($\Phi = 0.93$ *to* 1.24) and Table 2 ($\Phi = 1.24$ *to* 1.53).

In Table 1 and Table 2, P is P-Value that denotes the significance and the result is significant when $P < 0.05$. P_S and P_C are the P-Value of spatial and color characteristics, respectively. The β_S and β_C denote the regression coefficient of spatial and color characteristics, and β_0 is the common intercept of the *MLR* model. It can be seen from Table 1 and Table 2 that the model constructed with A_f, H_f and T_f is the same as with A_f, H_f and I_f, which is because the trends and distributions of T_f and I_f are almost identical, and the values of T_f and I_f are almost identical after data normalization.

Table 1. Parameters of the model and test results ($\Phi = 0.93$ *to* 1.24).

Selection	*Af, Tf*	*Af, If*	*Hf, Tf*	*Hf, If*
R2	0.9978	0.9978	0.9964	0.9964
MAE	0.0047	0.0047	0.0048	0.0048
P_S	<0.0001	<0.0001	<0.0001	<0.0001
P_C	<0.0001	<0.0001	<0.0001	<0.0001
VIF	6.4059	6.4059	5.9065	5.9065
β_S	-0.0632	-0.0632	-0.0859	-0.0859
β_C	-0.3302	-0.3302	-0.3413	-0.3413
β0	1.3162	1.3162	1.3202	1.3202

$$\Phi = -\,0.0632A_f - 0.3302I_f + 1.3162 \tag{13}$$

Table 1 indicates that the *Multi-dimensional-*Φ with A_f and T_f, I_f shows better performance in R^2 and *MAE*, and the relationship is formed as (13). It demonstrates that the variation of A_f is negatively correlated with Φ and the variations of T_f, I_f are negatively correlated with Φ under conditions ($\Phi = 0.93$ *to* 1.24). The relationships are consistent with the relationship between A_f and Φ in Fig. 4(a), and the relationship between T_f, I_f and Φ in Fig. 5(c) and Fig. 5(d).

Under normalized data conditions, the regression coefficients β_S and β_C indicate that the effect of a unit change in T_f or I_f on Φ is greater than that of a unit change in A_f on Φ. In other words, a change of one unit of Φ has a greater effect on A_f than on T_f and I_f. It also suggests that the introduction of spatial characteristics to construct the Φ

measurement model is feasible, in terms of both accuracy and sensitivity. Moreover, the *VIF* between A_f and I_G is 6.4059, which indicates that there is no severe multicollinearity between A_f and T_f, I_f.

Table 2. Parameters of the model and test results (Φ = *1.24 to 1.53*).

Selection	A_f, T_f	A_f, I_f	H_f, T_f	H_f, I_f
R^2	0.9978	0.9978	0.9964	0.9964
MAE	0.0035	0.0035	0.0042	0.0042
P_S	<0.0001	<0.0001	<0.0001	<0.0001
P_C	<0.0001	<0.0001	<0.0001	<0.0001
VIF	1.0599	1.0599	1.0718	1.0718
β_S	0.1676	0.1676	0.1807	0.1807
β_C	-0.6059	-0.6059	-0.5621	-0.5621
β_0	1.3698	1.3698	1.3602	1.3602

$$\Phi = 0.1676A_f - 0.6059I_f + 1.3698 \tag{14}$$

Similar to the initial conditions (Φ = *1.24 to 1.53*), a change of one unit of Φ has a greater effect on A_f than on T_f and I_f. It also suggests that the introduction of spatial characteristics to construct the Φ measurement model is feasible, in terms of both accuracy and sensitivity. And the *VIF* between A_f and T_f is 1.0599, which indicates that there is no severe multicollinearity between A_f and T_f, I_f.

The conventional *Color-Φ* model was constructed on normalized I_f and the relationship between Φ (Φ=*0.93 to 1.53*) and I_f is as (14). The data applied in the *Color-Φ* model are the same as in the *Multi-dimensional-Φ* model.

$$\Phi = -1.2728I_f^3 + 2.1773I_f^2 - 1.4956I_f + 1.4890 \tag{15}$$

C. Comparison with conventional Color-Φ model

The conventional Φ measurement model was constructed based on only color characteristics of flames, while an Φ measurement model that incorporates spatial and color information was proposed in the present paper. The same experimental data were processed by the conventional color-modelled Φ measurement model [8] and the improved color-modelled Φ measurement model [9] for further comparison. After all the data are normalized, the models proposed by Huang et al. [8] and Yang et al. [9] are almost the same. Therefore, we selected the model constructed on I_f as the *Color-Φ* model.

The *Multi-dimensional-Φ* model and the *Color-Φ* model were used to predict Φ of the testing set (each condition containing 20 random flame images), and the prediction is shown in Fig. 7. As a whole, the error between the predicted and true values of the *Multi-dimensional-Φ* model is smaller than the error between the predicted and true values of the *Color-Φ* model under conditions (Φ = *0.93 to 1.53*). The range of application of the *Color-Φ* model is limited, and it does not perform well except for conditions (Φ = *1.08* and *1.24*) in the experimental data compared with the *Multi-dimensional-Φ* model. In addition, the predicted values of the *Color-Φ* model fluctuate considerably under conditions (Φ = *0.93 to 1*), which indicates that the accuracy and stability of the *Color-Φ* model are not sufficient in these conditions.

Comparatively, the *Multi-dimensional-Φ* model has a good performance in accuracy and stability. To supply more direct insights, R^2 and *MAE* of the predicted values of the two models are shown in Table 3. It can be concluded from Table 3 that the R^2 and *MAE* of the *Multi-dimensional-Φ* model are smaller than those of the *Color-Φ* model, which indicates that the *Multi-dimensional-Φ* model has a better performance in terms of goodness of fit and the prediction errors on the test set.

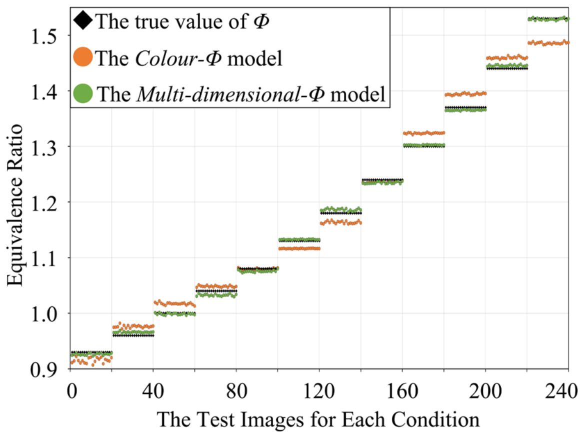

Fig. 7. Comparison of predicted values of *Color-Φ* and *Multi-dimensional-Φ* model.

In the predicted Φ values of the *Color-Φ* model and *Multi-dimensional-Φ* model, it can be found that the error of the model and the stability of the predicted values are relatively poor and unstable at Φ = *1.04*. It is because the flame speed of this condition is the highest in the whole condition (Φ = *0.93 to 1.53*). According to Mohammadreza et al. [17], for propane-oxygen-air flame (21% O2), freely propagating flame speed increases in slightly fuel-rich conditions, and the combustion frequency is the highest in this condition. In the progress of the combustion, the violent reaction of the flame causes certain fluctuations in the color characteristics and spatial characteristics of the flame, which lead to instability in the predicted values of the model. In addition to this, another reason for the large errors and fluctuations in the model at Φ = *1.04* is that the relationship between I_G and Φ is not completely linear in practice (Φ = *0.93 to 1.24*) but is only treated as an approximately linear relation in the *MLR* modelling process.

Table 3. The R^2 and *MAE* of the two models.

Model	R^2	*MAE*
Color-Φ	0.9886	0.0169
Multi-dimensional-Φ	0.9993	0.0043

CONCLUSION

In this work, the relationships between Φ and spatial, color characteristics have been investigated, which are nearly linear at conditions (Φ = *0.93 to 1.24* and Φ = *1.24 to 1.53*). Regarding the color modelled measurement of premixed air-propane flames under conditions (Φ = *0.93 to 1.53*), intensities of I_B and I_G were extracted as characteristics of the color space. Furthermore, T_f and I_f were extracted and they were approximately linearly correlated with the variation of Φ. A_f and H_f were extracted as the spatial characteristics, which showed a nearly linear varying trend to the variation of Φ.

The improved Φ measurement model of premixed propane flame was proposed, which takes both spatial and color characteristics into consideration. We have improved the accuracy and stability of the Φ measurement model using both color-spatial characteristics of digital color flame images. R^2 and *MAE* of the *Multi-dimensional-*Φ model were compared with those of the *Color-*Φ model. The comparison indicated that both the accuracy and stability of the *Multi-dimensional-*Φ model were better than the *Color-*Φ model. The proposed Φ measurement model provides a new modelling method in which all the characteristics varying with the independent can be considered. In addition, the rapid development of machine learning provides the possibility to fit multi-dimensional characteristics.

When applying this method to different fuel flames, the relationship between Φ and characteristics should be investigated in advance. And the relation should be approximately linear, which is the assumptions of the *MLR* model. Furthermore, according to the assumptions of *MLR* there must not be significant multicollinearity between the characteristics. Thus, the processing of the data is also one of the main tasks in the modelling process. However, the relationship between Φ and characteristics of flames is often not linear, and thus the application of *MLR* is limited to non-linear conditions. For the non-linear case, more non-linear machine learning algorithms can be applied to model Φ according to different requirements.

ACKNOWLEDGMENT

This work was supported by the Scientific Research Foundation of Guizhou Province (Grant No. [2022]133), the Industrial Project of Guizhou province (No. Qiankehe Zhicheng [2022]017), and Innovation group of Guizhou Education Department (No. Qianjiaohe KY [2021]012).

REFERENCES

[1] Turns, S.R. (2012). *An introduction to Combustion: Concepts and Applications. Third Edition*. McGraw-Hill. ISBN 978-0-07-338019-3.

[2] Brockhinke, A., Krüger, J., Heusing, M. (2012). Measurement and simulation of rota-tionally-resolved chemiluminescence spectra in flames. *Applied Physics B*, 107 (3), 539-549. https://www.doi.org/10.1007/s00340-012-5001-1

[3] Yang, J., Gong, Y., Guo, Q., Zhu, H., Wang, F., Yu, G. (2020). Experimental studies of the effects of global equivalence ratio and CO2 dilution level on the OH* and CH* chemiluminescence in CH4/O2 diffusion flames. *Fuel,* 278, 118307. https://www.doi.org/10.1016/j.fuel.2020.118307

[4] Kojima, J., Ikeda, Y., Nakajima, T. (2000). Spatially resolved measurement of OH^*, CH^*, and $C2^*$ chemiluminescence in the reaction zone of laminar methane/air premixed flames. *Proceedings of the Combustion Institute*, 28 (2), 1757-1764. https://www.doi.org/10.1016/S0082-0784(00)80577-9

[5] Clark, T. P. (1958). *Studies of OH, CO, CH, and C (sub 2) radiation from laminar and turbulent propane-air and ethylene-air flames*. Technical Note 4266, NACA, Washington, DC, US.

[6] Navakas, R., Saliamonas, A., Striugas, N., Džiugys, A., Paulauskas, R., Zakarauskas, K. (2018). Effect of producer gas addition and air excess ratio on natural gas flame luminescence. *Fuel*, 217, 478-489. https://doi.org/10.1016/j.fuel.2017.12.094

[7] Baumgardner, M.E., Harvey, J. (2020). Analyzing OH*, CH*, and C2* chemiluminescence of bifurcating FREI propane-air flames in a micro flow reactor. *Combustion and Flame*, 221, 349-351. https://doi.org/10.1016/j.combustflame.2020.08.009

[8] Huang, H.W., Zhang, Y. (2008). Flame colour characterization in the visible and infrared spectrum using a digital camera and image processing. *Measurement Science and Technology*, 19 (8), 085406. http://dx.doi.org/10.1088/0957-0233/19/8/085406

[9] Yang, J.S., Ma, Z., Zhang, Y. (2019). Improved colour-modelled CH* and C2* measurement using a digital colour camera. *Measurement*, 141, 235-240. https://doi.org/10.1016/j.measurement.2019.04.016

[10] Ge, H., Li, X.L., Li, Y.J., Lu, G., Yan, Y. (2019). Biomass fuel identification using flame spectroscopy and tree model algorithms. *Combustion Science and Technology*, 193 (6), 1-18. https://doi.org/10.1080/00102202.2019.1680654

[11] Quinlan, J. R. (1986). Induction of decision trees. *Machine Learning*, 1 (1), 81-106. https://www.doi.org/10.1023/A:1022643204877

[12] Breiman, L. (2001). Random forests. *Machine Learning*, 45 (1), 5-32. https://doi.org/10.1023/A:1010933404324

[13] Wang, Y., Yu, Y. F., Zhu, X. L., Zhang, Z. X. (2020). Pattern recognition for measuring the flame stability of gas-fired combustion based on the image processing technology. *Fuel*, 270, 117486. https://doi.org/10.1016/j.fuel.2020.117486

[14] Yang, J., Mossa, F. M. S., Huang, H. W., Wang, Q., Wolley, R., Zhang, Y. (2015). Oscillating flames in open tubes. *Proceedings of the Combustion Institute*, 35 (2), 2075-2082. https://doi.org/10.1016/j.proci.2014.07.052

[15] Mason R. L., Gunst, R. F., Hess J. L. (2003). *Statistical Design and Analysis of Experiments: With Applications to Engineering and Science. Second Edition*. John Wiley & Sons, ISBN 9780471372165.

[16] Hocking, R. R. (1976). A Biometrics invited paper. The analysis and selection of variables in linear regression. *Biometrics*, 32 (1), 1-49. https://doi.org/10.2307/2529336

[17] Baigmohammadi, M., Tabejamaat, S., Faghani-Lamraski, M. (2017). Experimental study on the effects of mixture flow rate, equivalence ratio, oxygen enhancement, and geometrical parameters on propane-air premixed flame dynamics in non-adiabatic meso-scale reactors. *Energy*, 121, 657-675. https://doi.org/10.1016/j.energy.2017.01.057

Received June 13, 2022
Accepted August 22, 2022